2011 IEEE/ACM Second International Conference on Cyber-Physical Systems

An Ultra Low Power Granular Decision Making using Cross Correlation: Minimizing Signal Segments for Template Matching

Hassan Ghasemzadeh, Roozbeh Jafari
Embedded Systems and Signal Processing Lab
Department of Electrical Engineering
Univeristy of Texas at Dallas, Richardson, TX 75080–3021
Email: {h.ghasemzadeh, rjafari}@utdallas.edu

Abstract*—Wearable sensor platforms have proved effective in a large variety of new application domains including wellness and healthcare, and are perfect examples of cyber physical systems. A major obstacle in realization of these systems is the amount of energy required for sensing, processing and communication, which can jeopardize small battery size and wearability of the entire system. In this paper, we propose an ultra low power granular decision making architecture, also called screening classifier, that can be viewed as a tiered wake up circuitry. This processing model operates based on simple template matching. Ideally, the template matching is performed with low sensitivity but at very low power. Initial template matching removes signals that are obviously not of interest from the signal processing chain keeping the rest of processing modules inactive. If the signal is likely to be of interest, the sensitivity and the power of the template matching blocks are gradually increased and eventually the microcontroller is activated. We pose and solve an optimization problem to realize our screening classifier and improve the accuracy of classification by dividing a full template into smaller bins, called mini-templates, and activating optimal number of bins during each classification decision. Our experimental results on real data show that the power consumption of the system can be reduced by more than 70% using this intelligent processing architecture. The power consumption of the proposed granular decision making module is six orders of magnitude smaller than state-of-the-art low power microcontrollers.

***Keywords*-Embedded Systems, Healthcare, Body Sensor Networks, Signal Processing, Power Optimization.**

I. Introduction

Lightweight wearable computers, also called Body Sensor Network (BSNs) or Body Area Networks (BANs), bring to fruition many opportunities to continuously monitor the human body with sensors placed on body or implanted in the body. These platforms revolutionize many application domains including healthcare and wellness applications. Examples of such applications include rehabilitation [1], sports medicine [2], geriatric care [3], gait analysis [4], diagnosis of obesity and depression [5, 6], and detection of neurodegenerative disorders such as Alzheimer's [7], Parkinson's [8], and Huntington's [9] diseases. Lightweight wearable computers are perfect examples of cyber physical systems where lightweight embedded computers are tightly coupled with the physical world (i.e. human body). In the past few years, new wearable applications have evolved and proved to be effective. Yet, one of the major obstacles is the size and weight of the sensor units. Smaller wearable units can enhance comfort and compliance. Smaller implantable units can enable many new applications. Battery size has been the dominating factor in the size of the sensors. Batteryless units operating on piezo, or units that require significantly smaller batteries, are not currently possible. The proposed technique in this paper aims to significantly reduce the power consumption of wearable units, and specifically the processing architecture.

Wearable sensor units are often composed of sensors, a processing unit (e.g. a microcontroller), a communication unit and a battery. Our current focus is on wearable motion sensors that are used for detection of human actions such as 'Sit to Stand' or 'Lie to Sit'. We propose an architecture, equipped with a *granular decision making module* (GDMM), that monitors incoming signals/actions. The granular decision making module attempts to detect actions that are not of interest as early as possible while consuming the least amount of energy. If the incoming action is likely to be of interest, the module will turn on the main signal processing unit (e.g. the microcontroller) for further processing. The granular decision making is done in a sequence of coarse to fine grained operations. At the beginning, the *screening* or preliminary signal processing may not exhibit high accuracy for classifying the incoming actions, but operates at an ultra low power. The objective of the initial screening is to identify *incoming actions* that are *obvious* rejects or accepts. As the module begins to observe the incoming actions that are *likely* of interest, more accurate decision making and screening processes are activated. Intuitively, screening at the beginning is done by a classification module with tunable parameters adjusted to consume the least amount of energy (e.g. by observing fewer samples with smaller bit resolution). The tunable parameters are adjusted to enhance the accuracy of signal processing and classification as the incoming signal or incoming action travels through screening blocks in the GDMM. The tunable parameters include time duration of actions, number and location of samples within each action, and bit resolution of sampled data. Collectively, screening blocks can select any combination of these transformations to adjust processing (or power) vs. accuracy. The decision making is performed in this fashion because often the incoming action is so dissimilar to the *action of interest* (also called target action) that it can be rejected even with a coarse-grained signal processing. For incoming actions that the screening block cannot reject with high confidence levels, the main signal processing unit will be activated. The main advantage of this method is the power saving due to removing actions that are not of interest from the signal processing chain as early as possible, deactivating the remaining modules in the signal processing chain.

Applications of healthcare monitoring have unique properties motivating our proposed technique: *Events of interest* often occur with a low duty cycle (e.g. $< 1\% - 5\%$) and the randomness to the incoming signals, even in cases where the signals are not of interest, is not significant. This assumption holds for many wearable applications where the objective is to detect sparse events such as walking, using motion sensors, [10–13], cardiac arrest [14, 15] and seizures, [16, 17] using implantable sensors. We utilize these unique properties of the applications and the physical world to reduce the power consumption by orders of magnitude in the cyber world. Although in our approach, every effort will be taken to ensure that granular decision making module provides acceptable precision in signal processing, in the events where it generates *false positives*, the sole drawback is the energy consumed to wake up the main signal processing unit for improved precision. Finally, the events are captured with a low sampling rate (e.g. $\leq 100Hz - 1kHz$) which implies that the processing can also be done at a slow speed. Unlike Wireless Sensor Networks (WSNs), wearable sensors often observe the same phenomenon, but with different *angles of view*. The data fusion approach in wearable computers is analogous to collaborative image processing in vision where a number of cameras are placed around the room and observe the same phenomenon, but with different angles of view. In WSNs, however, sensors are spread over a large area and often only a small number of sensors capture an event.

II. Related Works

Several ultra low power wearable systems, with signal processing capabilities, at the power budget of less than hundreds of μW have been proposed. The proposed systems, however, are either not programmable (except that they may provide a few tunable parameters), or the programmability is handled completely by a microcontroller. An intraocular CMOS pressure sensor system implant was proposed which contains an on-chip micro mechanical pressure sensor array, a temperature sensor, a microcontroller-based digital control unit, and an RF transponder [18]. An interface chip for implantable neural recording was proposed with tunable band-pass filters and adjustable gain [17]. A batteryless accelerometer system, that has a 3D loop antenna and utilizes the radio wave for power feeding was proposed. However, the control unit of the system is a microcontroller and it is unclear how it can be powered up by radio wave power feeding [19].

Several other systems were suggested that are primarily tailored towards specific applications, and are not generalizable. Examples include a machine-learning based patient-specific seizure detector [20], an implantable blood pressure sensor, an ECG sensing microsystem with adaptive RF powering [15, 21–23], an implantable batteryless telemetric microsystem for EMG recording [24] and a batteryless MEMS implant for cardiovascular applications [25].

III. Preliminaries

In this section, we present major hardware/software components of a typical BSN platform. Our focus in this work is on movement monitoring applications that use inertial information to examine human motions for the purpose of patient monitoring, diagnosis and treatment. However, the proposed methodology can be applicable to many other monitoring domains (e.g. a pacemaker that is required to detect abnormal ECG signals).

A. Sensor Nodes

A BSN is composed of several sensor nodes mounted on the patient's body, embedded with the clothing, or implanted in the human body. For the purpose of movement monitoring, motion sensor nodes are utilized. In our platform, each node has a microcontroller (i.e. TI MSP430) for signal processing, and a custom-designed sensor board including a 3-axis accelerometer and a 2-axis gyroscope for capturing inertial information. The sensor node has also a radio module for communication with other sensor nodes in the network or with a gateway such as a cell phone.

B. Per-node Signal Processing

Each sensor node has a microcontroller which can sample motion sensors at a certain rate. The acquired signals need to undergo specific embedded signal processing tasks in order to make higher level interpretations of human movements. The goal of main signal processing chain (MSPC) is to extract useful information from sensor data. Frequently, this data is a high-level observation, such as "Is the subject running?" or "What is the stride length when the subject is walking?". In other words, the purpose of main signal processing is to provide a 'fully' SW programmable environment for development of 'highly' reliable signal processing technique for action detection/verification and extracting details from the signals (e.g. balance during 'sit to stand' when it occurs). Typically, signal processing tasks are imposed by the application of the BSN. However, a basic requirement of movement monitoring applications is to detect actions first, and perform additional processing next. This application is

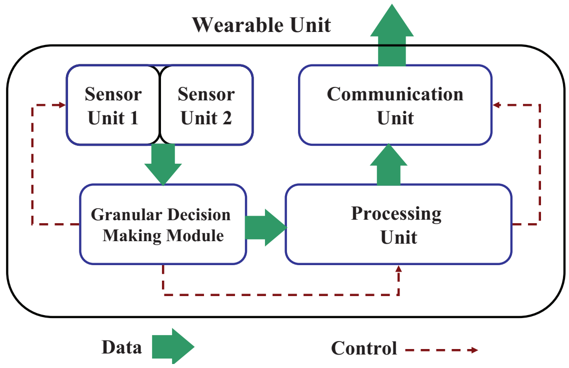

Figure 1. Overall system architecture illustrating granular decision making module (GDMM) in connection with communication unit, sensor units, and other computing modules.

usually referred to as *action recognition* [26–28]. Typical chain of signal processing for action recognition include filtering, segmentation, feature extraction, feature conditioning, and classification. The sampled data are first filtered to improve signal to noise ratio. A segmentation module [29–31] then separates portions of the signal that correspond to activities from those associated with rest (non-activity). The set of statistical features extracted from individual segments is reduced in size using feature conditioning techniques to speed up and enhance the classification task. At the end of the main signal processing chain (MSPC), a classifier (e.g. k-Nearest Neighbor [32]) is utilized to identify the action performed by the subject.

IV. Proposed Architecture

In many BSN applications, only a very small set of human actions is of interest. For example, gait analysis only is concerned with walking, fall detection with falls, Parkinson's disease monitoring with certain movements such as tremors, and sleep apnea with restless leg movements [33]. These target actions may occur infrequently. Considerable energy is wasted processing non-target actions. Efficiently rejecting non-target actions with a screening classifier could lead to a significant increase in system lifetime.

A. Granular Decision Making Module

An overall architecture of the proposed screening approach is illustrated in Figure 1. The granular decision making module (GDMM), which is composed of several coarse to fine grained screening classifiers, is responsible for screening sensor readings and activating main processing unit upon arrival of an event (e.g. action/movement) of interest.

Figure 2 shows block diagram of the proposed screening classifier operating based on template matching. There are two main components in the diagram, a granular decision making module, and the main signal processing block. The main signal processing is implemented on the main processor (e.g. microcontroller). The granular decision making module is an ultra low power screening classifier aiming to reject actions that are not of interest. This functionality is created by a multiplier-accumulator structure that implements a template matching function.

B. Template Matching

The screening classifier and the main signal processing form a rejecting chain of two classifiers. While the main signal processing uses classical patter recognition techniques to classify actions, the screening classifier employs simple template matching techniques to estimate the likelihood of occurrence of a target action. An unknown action is processed by the template matching block first. If the template matching block fails to reject the action, it is evaluated using the main signal processing block (i.e. the microcontroller). A template matching block functions as a binary classifier based on the cross correlation [34]. The incoming signal is compared to a predefined template of the target action. The comparison assigns a score value representing similarity between the current action and the template (target-action). The cross correlation score is then compared against a threshold and the action is either accepted or rejected. Only in case of acceptance the main signal processing is activated. The cross correlation measure was chosen because it can be implemented in HW by a series of multiplications and additions.

C. Tunable Parameters for Power Optimization

The template matching block described previously can be optimized for further energy saving by adjusting several tuning parameters. These parameters include time duration of actions considered for cross correlation calculation, number and location of samples, and bit resolution of data. This allows us to use a sequence of template matching blocks each contributing to the classification of events to certain level. The focus of this paper is on minimizing the number of samples used for calculation of the cross correlation function. Motivation behind this optimization is that even with a fixed bit resolution and action duration, only small portions of the template need to be considered when measuring similarity of an input signal with the template, hence the possibility to further save on the computations and energy consumption. We address this optimization problem by dividing a full template into several bins, each forming a *mini-template*. Mini-template approach will further reduce power consumption of the system allowing for realization of significantly less power-hungry wearable units that can eventually enable batteryless technologies for monitoring platforms. Furthermore, mini-templates highlight prominent patterns in the signal and eliminate irrelevant portions of the signal, and therefore, improve performance of signal processing and sensitivity of the classification system.

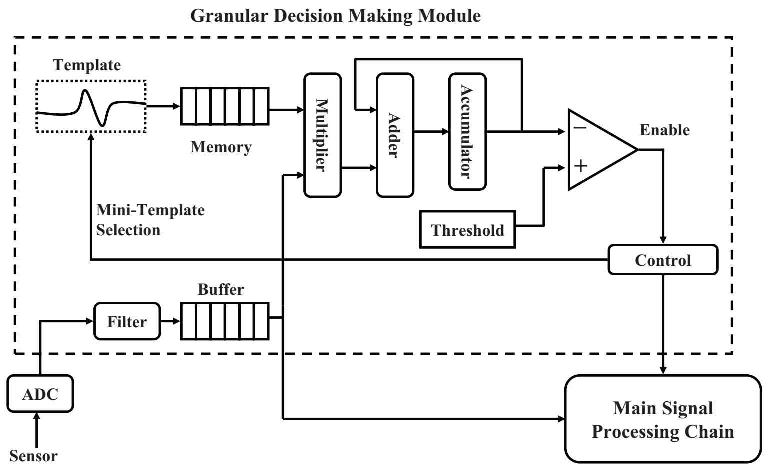

Figure 2. Block diagram of the granular decision making module (GDMM) and main signal processing chain (MSPC).

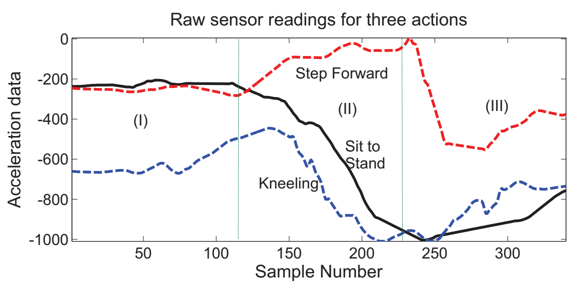

Figure 3. An example of three templates each divided into three mini-templates.

Figure 3 illustrates motivation behind using mini-templates. This figure shows real data collected with our wearable sensors where only three actions are used for visualization. The graphs show raw sensing readings from Z-axis accelerometer of a node placed on the ‘Waist’ of a subject. Assume ‘Sit to Stand’ (bold black plot) is the action of interest and the other two actions, ‘Kneeling’ (dashed blue plot) and ‘Step Forward’ (dashed red plot) may occur as non-target. Clearly, if the entire template is considered, the target action can be distinguished from the others based on the cross correlation measure. Assume each template is divided into three bins as indicated by (I), (II), and (III). None of the bins can solely achieve small false positive rates. For instance, if only bin (I) is used, a ‘Step Forward’ action may be classified as ‘Sit to Stand’ leading to high misclassification rate. Similarly, bins (II) and (III) are strongly correlated with the target action (‘Sit to Stand’) resulting in a large number of false positives. However, assume the case where only bins (I) and (II) are activated for template matching. The only action that can be accepted by both bins is ‘Sit to Stand’. If an action is accepted by bin (I), it can be confidently considered as either ‘Sit to Stand’ or ‘Step Forward’. If the action is further accepted by bin (II), the choice of ‘Step Forward’ is ignored leaving ‘Sit to Stand’ as the final classification decision. By activating only two bins rather than the entire template, one-third of the multiply-add operations are discarded from the template matching resulting in 33% savings. Therefore, our objective is to find a minimum subset of template bins that can confidently activate the main signal processing block while maintaining low false positive rates. We note that the ordering of processing mini-templates is also important because a suboptimal ordering can result in a larger number of bins being processed.

V. Minimum Size Mini-Template Set

As discussed in previous section, the template matching block in Figure 2 can be divided into several lower cost blocks associated with a set of predefined mini-templates. We pose an optimization problem that finds the minimum subset of template bins and their ordering required for detection of a target action subject to a given upper bound on the false positive rates. We call this optimization problem *Minimum Size Mini-Template Set* (MSMTS). Throughout this section, we use the notations in Table I to formulate this problem.

A. Template Generation

Given a target action $\hat{a}$ and $A = \{a_1, a_2, \ldots, a_n\}$ a set of n non-target actions, we generate templates $\hat{T}$, and $\{T_1, T_2, \ldots, T_n\}$ from a set of training trials. Templates are generated as shown in Definition 2 according to the similarity score between training trials. The MSMTS problem constructs a decision path using properties of these templates.

***Definition** 1 (Similarity Score):* Given two time series signals f and g of length N, the similarity score $\gamma(f,g)$ between the two signals is defined based on their normalized

Table I
NOTATIONS

Term	Description
$\hat{a}$	target action
A	set of n not-target actions
a_i	i-th non-target action
a_i^l	l-th training trial of action a_i
T_i	template generated for action a_i
K	number of template bins
B	set of template bins due to template partitioning
b_k	k-th template bin due to template partitioning
MT_{ik}	k-th mini-template of a_i associated with b_k
$\gamma(T_i, T_j)$	similarity score between templates T_i and T_j
O	optimal subset of bins used for classification
R	size of optimal set O found by MSMTS problem

cross correlation by

$$\gamma(f,g) = \frac{\sum_{t=1}^{N}[f(t)-\bar{f}][g(t)-\bar{g}]}{\sqrt{\sum_{t=1}^{N}[f(t)-\bar{f}]^2 \sum_{t=1}^{N}[g-\bar{g}]^2}} \tag{1}$$

where $\bar{f}$ and $\bar{g}$ denote mean values of f and g.

***Definition** 2 (Template):* Given an action a_i with L training trials, a template T_i for a_i is the best representative trial with respect to the similarity score γ between all pairs of trials. The trial with the highest summed similarity score between itself and the other trials is selected, as shown in (2).

$$T_i = \arg\max_{a_i^l} \sum_r \gamma(a_i^l, a_i^r) \tag{2}$$

Each template is evenly divided into K bins $B = \{b_1, b_2, \ldots, b_K\}$. Each bin b_k represents a set of mini-templates associated with target action and different non-target actions. We investigate how each one of the bins contributes to detection of a target action and choose the best sequence of template bins to be examined during template matching.

B. Problem Formulation

In this section, we formally define MSMTS problem.

***Definition** 3 (Weakly Correlated):* Within each bin b_k, an action a_i is referred to as weakly correlated with the target action if $\gamma(\hat{MT}_k, MT_{ik}) < 1 - \epsilon_k$, where $\hat{MT}_k$ is the k-th mini-template associated with target action $\hat{a}$ and MT_{ik} denotes the k-the mini-template associated with a_i. Similarly, for each bin b_k, a set WCS_k, *Weakly Correlated Set*, is defined as the set of actions that are weakly correlated.

The value of ϵ_k is a design parameter which determines the accuracy of the system. Higher values of ϵ_k represent higher likelihood of match with target action, resulting in higher true positive rates and lower false positive rates. In fact, $thr_k = 1 - \epsilon_k$ is the threshold (see Figure 2) for acceptance/rejection of incoming signals. Intuitively, an incoming signal that is weakly correlated in b_k will be rejected. The signal, however, will be further processes by subsequent bins if it is accepted by a bin b_k on the decision path. Clearly, in order to accept an event, it needs to be weakly correlated with all non-target actions.

***Definition** 4 (Complete Ordering):* An ordering O=$\{b_1, b_2, \ldots, b_R\}$ is complete if the following condition holds.

$$\bigcup_{k=1}^{R} WCS_k = A \tag{3}$$

***Definition** 5 (Ordering Cost):* Let O=$\{b_1, b_2, \ldots, b_R\}$ be a complete ordering of sensor nodes and $f(a_i)$ a function that gives the index of the first bin in which the following condition holds:

$$\{a_i \mid a_i \in A\} \quad \subset \quad \bigcup_{k=1}^{f(a_i)} WCS_k \tag{4}$$

That is, $f(a_i)$ is the number of bins that need to be examined in order to reject a_i. Then the total cost of the ordering is given by the following equation:

$$Z = \sum_{a_i \in A} f(a_i) \tag{5}$$

***Problem** 1 (Min Size Mini-Template Set):* Given a finite set A and WCS, where WCS=$\{WCS_1, WCS_2, \ldots, WCS_K\}$ is a collection of subsets of A such that the union of all WCS_i forms A, MSMTS is the problem of finding a complete linear ordering such that the cost of the ordering is minimized.

C. Problem Complexity

Through the following theorem, we prove that the MSMTS problem is NP-hard.

***Theorem** 1:* The Min Size Mini-Template Set problem is NP-hard.

Proof: It is straightforward to see that Min Sum Set Cover (MSSC) problem can be reduced to our MSMTS problem. The known MSSC problem is described as follows. Let U be a finite set of elements and S=$\{S_1, S_2, \ldots, S_m\}$ a collection of subsets of U such that their union forms U. A linear ordering of S is a bijection f from S to $\{1, 2, \ldots, m\}$. For each element $e \in U$ and linear ordering f, we define $f(e)$ as the minimum of $f(S)$ over all $\{S_i : e \in S_i\}$. The goal is to find a linear ordering that minimizes $\sum_e f(e)$. It is easy to see that by replacing elements of U with those of A, and also replacing subsets S_i with WCS_i we obtain the same problem as MSSC. Therefore, MSMTS is an NP-hard problem. ■

***Theorem** 2:* There exists no polynomial-time approximation algorithm for MSMTS with an approximation ratio less than 4.

Proof: Reducing MSSC problem to MSMTS preserves approximation of any corresponding solutions. Therefore, any lower bound for MSSC also holds for MSMTS. In [35], it is shown that for every $\varepsilon > 0$, it is NP-hard to approximate MSSC within a ratio of $4 - \varepsilon$. Therefore, 4 is also a lower bound on the approximation ratio of MSMTS. ■

Algorithm 1 Greedy solution for MSMTS

Calculate set WCS_k for every bin b_k
$O = \phi$
while $O \neq A$ **do**
  Select bin b_k such that WCS_k is maximum cardinality
  $O = O \bigcup b_k$
  for all $e \in WCS_k$ **do**
    remove e from all WCS_j (j={1,...,K})
  end for
end while

Table II
EXPERIMENTAL ACTIONS

No.	Action
1	Sit to Stand
2	Sit to Lie
3	Bend to Grasp
4	Kneel
5	Rise from Kneeling
6	Turn Clockwise
7	Step Forward
8	Step Backward
9	Jump

D. Greedy Solution

The greedy algorithm for MSMTS is adapted from the greedy algorithm for MSSC and is shown in Algorithm 1. At each step, it searches for the bin b_k that can reject largest number of remaining non-target events (by searching through the WCS_k). It then adds such a bin to the solution space O and removes the actions it can reject from further consideration. The algorithm terminates when all non-target actions are rejected. The approximation ratio is 4 as previously discussed.

VI. EXPERIMENTAL VERIFICATION

In order to demonstrate performance of the proposed signal screening approach, we carried out a set of experiments where three subjects were asked to perform the actions listed in Table II, each ten times. Each subject wore a set of seven sensor nodes, as described in Section III-A, secured to the upper and lower body segments as well as the 'Waist'. The nodes were programmed to sample five sensors including x, y, z accelerometer and x, y gyroscope at 50 Hz. The data were collected using a custom-designed MATLAB tool for further processing. We used 50% of the trials as training set for template generation and finding optimal decision path, and the remaining trials as test set for estimating the accuracy of the system in classifying actions.

A. Power Consumption of Screening Blocks

Our objective was to measure energy saving that can be obtained when one action is aimed to be the target action (i.e. identified & accepted) and the rest are considered as non-target. For each action, we generated a unique template as described in Section V-A. As discussed in Section IV-C, the power consumption of each screening block depends on several tunable parameters. In particular, the number of samples used for template matching can affect the power consumption significantly.

Table III
OPTIMAL ORDERING (DECISION PATH)

K	B (Bin Set)	Bin Length	Decision Path	Active Fraction (%)
2	$\{b_1,b_2\}$	150	$b_1 \rightarrow b_2$	100.0
5	$\{b_1,\ldots,b_5\}$	60	$b_2 \rightarrow b_1$	40.0
10	$\{b_1,\ldots,b_{10}\}$	30	$b_3 \rightarrow b_1$	20.0
15	$\{b_1,\ldots,b_{15}\}$	20	$b_3 \rightarrow b_5$	18.3
20	$\{b_1,\ldots,b_{20}\}$	15	$b_2 \rightarrow b_6$	17.0
25	$\{b_1,\ldots,b_{25}\}$	12	$b_2 \rightarrow b_8$	15.0
30	$\{b_1,\ldots,b_{30}\}$	10	$b_3 \rightarrow b_9$	13.3

To estimate power consumption of the template matching, the screening blocks were implemented using Multiplier-ACcumulator (MAC) units. MACs were designed using Verilog. The cross-correlation was enabled by a series of MAC steps depending on the number of incoming samples. At each clock instant, the digitized template data and the incoming signal data were multiplied and added to the previous MAC value. This continued, depending on the number of samples for the incoming event. The design was synthesized using Synopsys with the 45 nm NanGate Open Cell library. The simulations of the Verilog RTL were observed using Synopsys VCS. The switching activity was then considered and the power numbers were computed in Synopsys. The power values were then computed in a similar fashion for templates and mini-templates of different lengths on the incoming data.

B. Full-Template vs. Mini-Template

In the first step, we considered 'Sit to Stand' as target action and all other actions as non-target. The power consumption of a screening block with full size template was computed as discussed in Section VI-A. The power consumption of the full template screening block was 6.58 nW which is significantly smaller than the power consumption of a typical signal processing chain (e.g. power consumption of processing unit of a Telos mote 3 mW in active mode). We then divided the entire template into several bins and used the Min Size Mini-Template Set problem to find optimal ordering of the bins that are required for detecting 'Sit to Stand'. A template on Z-axis accelerometer is a vector of 300 samples that corresponds to 6 seconds of sensor readings. A choice of K=10 (for example) generates ten bins, each having a length of 30 samples. We solved our optimization problem (see Problem 1) using the greedy algorithm described in Algorithm 1. Ideally, only a small subset of the bins would suffice for reliable identification of the target action. Table III shows optimal ordering of the active bins (decision path) for different number of bins (K), ranging from 2 to 30. The last column shows the percentage

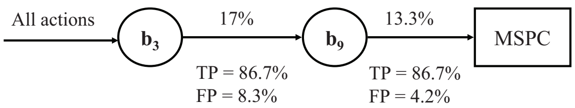

Figure 4. Decision path and accuracy in terms of acceptance rate of individual screening blocks for the case of K=30. Resulting path has only two screening blocks associated with 3rd and 9th mini-templates.

of the full template that needs to be active during processing. A more detailed illustration of decision path for the case of 30 bins is given in Figure 4. This decision path has only two screening blocks, b_3 and b_9. Out of all incoming action trials, 83% are rejected by b_3 resulting in 17% of the movements being passed to the next screening block, b_9. This last screening block will reject another 3.7% of the trials leaving only 13.3% being processing by MSPC. Figure 4 also shows accuracy of the decision path in terms of true positive and false positive rates.

Figure 5(a) shows power consumption of the template matching architecture. We recall that when a larger number of false positives can be tolerated, smaller number of template bins is needed for signal screening, resulting in consuming less power by the screening blocks. The reason is that with a high false positive, each individual bin b_k can interpret more non-target actions as being weakly correlated with the target action. Therefore, less bins are needed to form a complete ordering (see Definition 4). In our experiments, we observed that with 20% false positive rate, two template bins (see fourth column in Table III) were detected by our greedy algorithm to be on the decision path. However, only one template bin was active when a 50% false positive rate is considered. We note, however, that higher false positives will result in more actions being processed by the main processor which results in overall higher power consumption of the entire system due to significantly higher power consumed by the microcontroller. Furthermore, the number of active bins is fixed (i.e. 2 for FP=0.2 & 1 for FP=0.5) when the number of bins grows. Therefore, the amount of power consumption reduces as the number of bins increases (see Figure 5(a)) because the individual bins get smaller. This confirms our intuition that only a small fraction of the template can be used for signal screening. Overall, the amount of power consumption ranges from 6.58 nW for $K = 2$ (two template bins) with 20% false positive, to 0.23 nW for $K = 30$ with 50% false positive rate.

We also compared the power consumption of the decision paths (multiple screening blocks with mini-templates) with that of a full template (i.e. 6.58 nW) to highlight the amount of extra power reduction made by the mini-template structure. Figure 5(b) shows percentage of improvement in power optimization achieved by our optimization problem (as proposed in Section V). We note that if the full template is divided into small number of bins (e.g. $K = 2$) most

Table IV
POWER SAVING

		W/o Screening	W/ Screening
FP=0.2	Processor Activation	100%	29%
	Power (Processor)	3 mW	0.87 mW
	Screening Activation	-	100%
	Power (Screening)	-	1.87 nW
	Power Saving	-	71%
FP=0.5	Processor Activation	100%	56%
	Power (Processor)	3 mW	1.68 mW
	Screening Activation	-	100%
	Power (Screening)	-	0.93 nW
	Power Saving	-	44%

of the bins might be on the decision path, which results in small improvement. Therefore, it is important to divide the template into a sufficiently large number of bins (K) and find only a small number of bins (R) for screening as suggested by the Min Size Mini-Template Set problem. In our experiments, a ratio of 10% between length of mini-templates and length of full-template (e.g. 30 and 300 for 'Sit to Stand') leaves sufficient information within each mini-template for classification. Therefore, the number of bins can be set to satisfy this requirement. As suggested in Figure 5(b), we obtained an average improvement of 78.7% with mini-templates for detecting 'Sit to Stand'.

The power consumption of the proposed screening classifier was compared with that of an MSP430 microcontroller which consumes 3 mW in active mode. Table IV shows overall power consumption of both screening blocks and main processor (where main signal processing is running) as well as the amount of power savings obtained due to using screening blocks. In particular, 71% power saving was achieved when only 20% of the non-target actions are accepted by the screening blocks (FP=0.2). The amount of power savings that can be achieved by our screening approach highly depends on the frequency of occurrence of the target action. For our experiments, we assumed that all actions are equally likely, and therefore, 'Sit to Stand' occurs 11% of the times. In reality, however, human actions are sparse occurring a lot more infrequently, which results in much higher power savings.

C. Per-Action Screening

In order to measure the power consumption of our system for screening individual actions listed in Table II, we consider each action as target, and find minimum number of mini-templates needed for screening that particular action. The value of acceptance/rejection threshold (see Definition 3) was set to guarantee a maximum false positive rate of 20%. We repeated this test for different values of K (number of template bins) only including 10, 20, and 30 which the decision path was detected by the greedy algorithm. Figure 6(a) shows the total power consumption of the active screening blocks, which ranges from 0.23 nW to 1.45 nW with an average of 0.85 nW over all the experiments. The

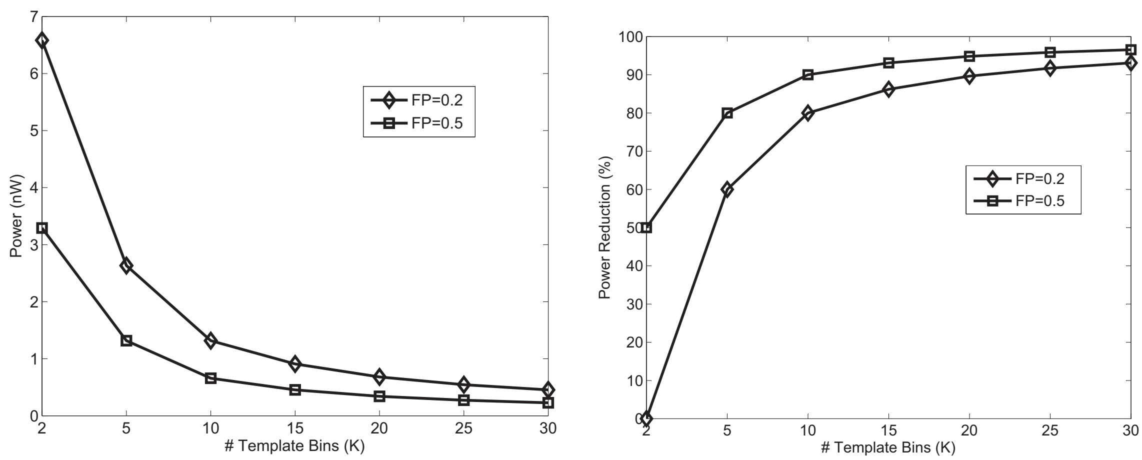

(a) Power Consumption (b) Power Reduction

Figure 5. Power consumption of screening blocks (a), improvement in power reduction obtained by mini-templates (b), while Z-axis accelerometer of 'Waist' node is used for screening 'Sit to Stand' movements.

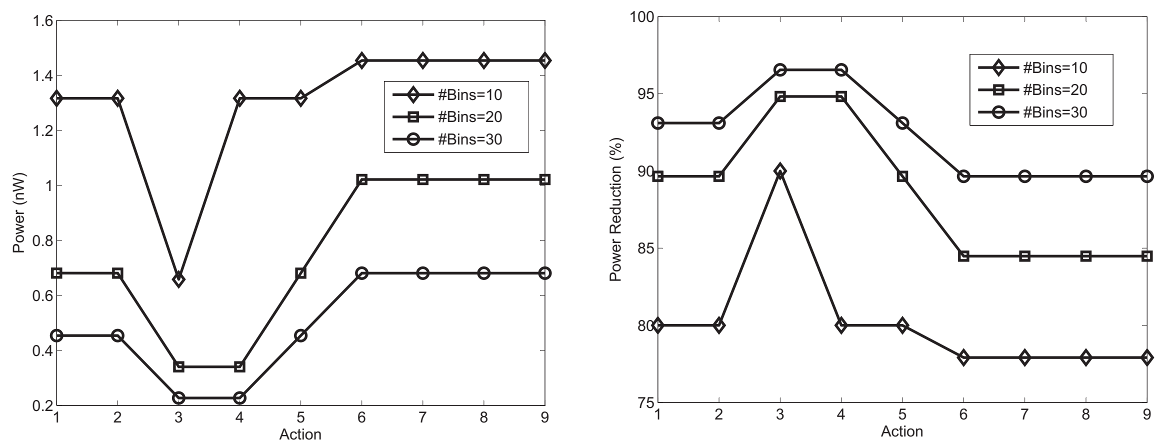

(a) Power Consumption (b) Power Reduction

Figure 6. Power consumption of screening blocks (a), and improvement over full size template architecture (b), upper bound on false positive rate is set to be 20%.

small power consumption for detecting action 3 ('Bend to Grasp') compared to other actions can be interpreted as follows. The sensor node used for screening 'Bend to Grasp' actions is 'Right Wrist' which has significantly different pattern during this action compared to other actions. Thus, a smaller number of bins (shorter decision path) is enough to perform preliminary signal screening. In contrast, a 'Waist' node, for example, may experience similar patterns during 'Sit to Stand' and 'Rise from Kneeling', and therefore, more screening blocks are required to reliably accept/reject the incoming actions. Figure 6(b) shows percentage of improvement in power consumption of the screening blocks, over a full template screening block, made by the optimization problem. Improvements range from 77.9% for 'Turn Clockwise' action with 10 template bins to 96.6% for 'Bend to Grasp' action with 30 bins. The average improvement achieved was 87.0%. Furthermore, the amount of energy saving obtained with this experiment was 71.1%.

D. Accuracy

In order to measure accuracy of the optimal mini-template set in classifying a target action, we used only the mini-templates determined by our greedy optimization algorithm while an incoming signal is accepted if it is accepted by all screening blocks. Our goal was to estimate sensitivity of the template matching architecture while acceptance threshold is already set during training. This test resulted in a true positive rate of 93.3% on average.

VII. Discussion and Future Work

We used cross-correlation scores to perform preliminary low power signal processing by quantifying similarity between incoming signals and target action. This approach is promising and allows for significant power saving while achieving acceptable true positive rates (e.g. 93.3%). Higher power savings can be obtained in the expense of increase in false positive rates. In order to maintain smaller false positive rates, more complicated computing blocks (as alternatives for cross-correlation) can be used. Clearly, there are tradeoffs between complexity of screening blocks and desired false positive rates. Currently, we are investigating alternative similarity measures for cross-correlation, and studying different system design tradeoffs.

In our experiments, we assumed that experimental actions occur continuously and at equal frequencies. In reality, however, human actions can be sparse, occurring at significantly lower rates. This will allow for activating the main processing less frequently, and therefore, saving more power.

Our work on designing granular decision making architectures for wearable platforms is ongoing. We are currently investigating refinement of the template matching blocks for further optimization with respect to other tunable parameters such as bit resolution of sensor readings and duration of incoming actions. We are also exploring this approach in the frequency domain.

VIII. Conclusion

In this paper, we proposed an ultra low power signal screening methodology for power optimization in lightweight embedded systems and demonstrated the effectiveness of our approach for energy saving in healthcare domain as an example of cyber physical systems. Our signal screening model operates based on a series of template matching blocks. Each screening module is associated with a small portion of a predefined template, called mini-template. Our signal screening approach rejects actions that are unlikely to be the target action and activates the main processor only if the incoming signal is highly correlated with the template and is likely a target action. The proposed hardware-assisted algorithm can be used to significantly reduce energy consumption of wearable sensory platforms such as those used in healthcare applications. Our experimental results demonstrate the effectiveness of the proposed architecture in reducing the power consumption of the system. In particular, we achieved energy savings of more than 70% for screening different transitional movements involved in our daily lives.

References

[1] E. Jovanov, A. Milenkovic, C. Otto, and P. de Groen, "A wireless body area network of intelligent motion sensors for computer assisted physical rehabilitation," *Journal of NeuroEngineering and Rehabilitation*, vol. 2, no. 1, p. 6, 2005.

[2] W. Jones, "Helmets sense the hard knocks [news]," *Spectrum, IEEE*, vol. 44, no. 10, pp. 10–12, Oct. 2007.

[3] J. Chen, K. Kwong, D. Chang, J. Luk, and R. Bajcsy, "Wearable sensors for reliable fall detection," *Engineering in Medicine and Biology Society, 2005. IEEE-EMBS 2005. 27th Annual International Conference of the*, pp. 3551–3554, Jan. 2005.

[4] S. Morris and J. Paradiso, "Shoe-integrated sensor system for wireless gait analysis and real-time feedback," *[Engineering in Medicine and Biology, 2002. 24th Annual Conference and the Annual Fall Meeting of the Biomedical Engineering Society] EMBS/BMES Conference, 2002. Proceedings of the Second Joint*, vol. 3, pp. 2468–2469 vol.3, Oct. 2002.

[5] A. Cooper, A. Page, K. Fox, and J. Misson, "Physical activity patterns in normal, overweight and obese individuals using minute-by-minute accelerometry," *European journal of clinical nutrition*, vol. 54, no. 12, pp. 887–894, 2000.

[6] E. Naujokat, M. PERKUHN, M. Harris, and C. Norra, "Depression detection system," June 2006, wO Patent WO/2006/056,907.

[7] A. Pettersson, M. Engardt, and L. Wahlund, "Activity level and balance in subjects with mild alzheimer's disease," *Dementia Geriatric Cognitive Disorders*, vol. 13, pp. 213–216, 2002.

[8] S. L. Mitchell, J. J. Collin, C. J. D. Luca, A. Burrows, and L. A. Lipsitz, "Open-loop and closed-loop postural control mechanisms in parkinson's disease: increased mediolateral activity during quiet standing," *Neuroscience Letters*, vol. 197, no. 2, pp. 133 – 136, 1995.

[9] V. Emmerik and V. Wegen, "On the functional aspects of variability in postural control," *Exercise and Sport Sciences Reviews*, vol. 30, no. 4, pp. 177–183, 2002.

[10] K. O'Donovan, B. Greene, D. McGrath, R. O'Neill, A. Burns, and B. Caulfield, "Shimmer: A new tool for temporal gait analysis," in *Proceedings of the 31st Annual International Conference of the IEEE Engineering in Medicine and Biology Society: Engineering the Future of Biomedicine, EMBC 2009*, 2009, pp. 3826–3829.

[11] S. Hagler, D. Austin, T. Hayes, J. Kaye, and M. Pavel, "Unobtrusive and ubiquitous in-home monitoring: A methodology for continuous assessment of gait velocity in elders," *IEEE Transactions on Biomedical Engineering*, vol. 57, no. 4, pp. 813–820, 2010.

[12] Y. Ohta, N. Motooka, I. Siio, K. Tsukada, and K. Kambara, "Non-invasive gait monitoring in a ubiquitous computing house," *IEEJ Transactions on Electronics, Information and Systems*, vol. 130, no. 3, pp. 383–387+3, 2010.

[13] E. Guenterberg, A. Yang, H. Ghasemzadeh, R. Jafari, R. Bajcsy, and S. Sastry, "A method for extracting temporal parameters based on hidden markov models in body sensor networks with inertial sensors," *IEEE Transactions on Information Technology in Biomedicine*, vol. 13, no. 6, pp. 1019–1030, 2009.

[14] J. Vaisanen, J. Hyttinen, and J. Malmivuo, "Finite difference and lead field methods in designing implantable ecg monitor," *Medical and Biological Engineering and Computing*, vol. 44, no. 10, pp. 857–864, 2006.

[15] P. Cong, N. Chaimanonart, W. Ko, and D. Young, "A wireless and batteryless 10-bit implantable blood pressure sensing microsystem with adaptive rf powering for real-time laboratory mice monitoring," *IEEE Journal of Solid-State Circuits*, vol. 44, no. 12, pp. 3631–3644, 2009.

[16] F. Shahrokhi, K. Abdelhalim, D. Serletis, P. Carlen, and R. Genov, "The 128-channel fully differential digital integrated neural recording and stimulation interface," *IEEE Transactions on Biomedical Circuits and Systems*, vol. 4, no. 3, pp. 149–161, 2010.

[17] W.-S. Liew, L. Zou, X. abd Yao, and Y. Lian, "A 1-v 60-uw 16-channel interface chip for implantable neural recording," in *Proceedings of the Custom Integrated Circuits Conference*, 2009, pp. 507–510.

[18] K. Stangel, S. Kolnsberg, D. Hammerschmidt, B. Hosticka, H. Trieu, and W. Mokwa, "A programmable intraocular cmos pressure sensor system implant," *IEEE Journal of Solid-State Circuits*, vol. 36, no. 7, pp. 1094–1100, 2001.

[19] S. Sasaki, T. Seki, and S. Sugiyama, "Batteryless accelerometer using power feeding system of rfid," in *2006 SICE-ICASE International Joint Conference*, 2006, pp. 3567–3570.

[20] A. Shoeb, D. Carlson, E. Panken, and T. Denison, "A micropower support vector machine based seizure detection architecture for embedded medical devices," in *Proceedings of the 31st Annual International Conference of the IEEE Engineering in Medicine and Biology Society: Engineering the Future of Biomedicine, EMBC 2009*, 2009, pp. 4202–4205.

[21] P. Cong, N. Chaimanonart, W. Ko, and D. Young, "A wireless and batteryless 130mg 300?w 10b implantable blood-pressure-sensing microsystem for real-time genetically engineered mice monitoring," in *Digest of Technical Papers - IEEE International Solid-State Circuits Conference*, 2009.

[22] N. Chaimanonart and D. J. Young, "An adaptively rf-powered wireless batteryless in vivo ekg and core body temperature sensing microsystem for untethered genetically engineered mice real-time monitoring," in *INSS'09: Proceedings of the 6th international conference on Networked sensing systems*. Piscataway, NJ, USA: IEEE Press, 2009, pp. 52–57.

[23] P. Cong, W. Ko, and D. Young, "Wireless batteryless implantable blood pressure monitoring microsystem for small laboratory animals," *IEEE Sensors Journal*, vol. 10, no. 2, pp. 243–254, 2010.

[24] J. Parramon, P. Doguet, D. Marin, M. Verleyssen, R. Munoz, L. Leija, and E. Valderrama, "Asic-based batteryless implantable telemetry microsystem for recording purposes," in *Annual International Conference of the IEEE Engineering in Medicine and Biology - Proceedings*, vol. 5, 1997, pp. 2225–2228.

[25] N. Najafi and A. Ludomirsky, "Initial animal studies of a wireless, batteryless, mems implant for cardiovascular applications," *Biomedical Microdevices*, vol. 6, no. 1, pp. 61–65, 2004.

[26] H. Ghasemzadeh, E. Guenterberg, and R. Jafari, "Energy-Efficient Information-Driven Coverage for Physical Movement Monitoring in Body Sensor Networks," *IEEE Journal on Selected Areas in Communications*, vol. 27, pp. 58–69, 2009.

[27] H. Ghasemzadeh, J. Barnes, E. Guenterberg, and R. Jafari, "A Phonological Expression for Physical Movement Monitoring in Body Sensor Networks," in *Mobile Ad Hoc and Sensor Systems, 2008. MASS 2008. 5th IEEE International Conference on*, 2008, pp. 58–68.

[28] H. Ghasemzadeh, V. Loseu, and R. Jafari, "Structural action recognition in body sensor networks: Distributed classification based on string matching," *Information Technology in Biomedicine, IEEE Transactions on*, vol. 14, no. 2, pp. 425 –435, 2010.

[29] Z. Lin and L. Davis, "Shape-based human detection and segmentation via hierarchical part-template matching," *IEEE Transactions on Pattern Analysis and Machine Intelligence*, vol. 32, no. 4, pp. 604–618, 2010.

[30] T. Pfau, M. Ferrari, K. Parsons, and A. Wilson, "A hidden Markov model-based stride segmentation technique applied to equine inertial sensor trunk movement data," *Journal of Biomechanics*, vol. 41, no. 1, pp. 216–220, 2008.

[31] E. Guenterberg, H. Ghasemzadeh, and R. Jafari, "A Distributed Hidden Markov Model for Fine-grained Annotation in Body Sensor Networks," in *Proceedings of the 2009 Sixth International Workshop on Wearable and Implantable Body Sensor Networks-Volume 00*. IEEE Computer Society, 2009, pp. 339–344.

[32] R. O. Duda, P. E. Hart, and D. G. Stork, *Pattern Classification*. Wiley-Interscience Publication, 2000.

[33] M. Ohayon and T. Roth, "Prevalence of restless legs syndrome and periodic limb movement disorder in the general population," *Journal of psychosomatic research*, vol. 53, no. 1, pp. 547–554, 2002.

[34] J. Lewis, "Fast normalized cross-correlation," in *Vision Interface*, vol. 10, 1995, pp. 120–123.

[35] U. Feige and P. Tetali, "Approximating min sum set cover," *Algorithmica*, vol. 40, no. 4, pp. 219–234, 2004.